

1 **A Formal Model of Mood Disorders Based on the Neural Circuit**

2 **Dynamics of the Triple Network Model**

3 Alan Lawrence Rubin M.D. (no affiliation), 1233 Beech Street, Atlantic Beach, New York, 11509

4 516-695-5589, Fax: 516-431-8209, alawrencerubin@gmail.com

5 Mark Walth, PHD candidate, Department of Mathematics, Cornell University

6

7 **Abstract**

8 Psychiatric diagnoses are based on consensus and are not related to pathophysiology, leading to
9 confusion in treatment and in basic and clinical psychiatric research. The pathology of mood
10 disorders arises from the intrinsic function and interactions between key neural circuits of the
11 triple network. These circuits are the central executive network composed of the dorsolateral
12 prefrontal cortex and posterior parietal cortex; the default mode network consisting of the dorsal
13 medial prefrontal cortex, posterior cingulate/precuneus and angular gyrus and the salience
14 network made up of the anterior insula, dorsal anterior cingulate cortex associated with
15 subcortical limbic nodes including the amygdala. In this work, we develop a formal model using
16 nonlinear dynamics and network theory, which captures the dynamic interactions of these three
17 brain networks, allowing us to illustrate how various mood disorders can arise. Recurrent circuit
18 dynamics are modeled on the physio-dynamics of a single neural component and is dependent
19 on a balance of total input (feedforward and feedback) and the sensitivity of activation of its

20 neural components. We use the average percentage of maximal firing rate frequency as a
21 measure of network activity over long periods, which corresponds to fMRI activity.

22 While the circuits function at moderate rates in euthymia, depressive symptoms are due to
23 hypoactivity of the CEN and SN and hyperactivity of the DMN. Mania arises from a hyperactive
24 SN with hypofunction of the CEN and moderate to high activity of the DMN. Functional
25 abnormalities arise from genetic or epigenetic changes, affecting either the weight of neural
26 interconnections or the sensitivity of activation of neurons comprising the network. Decreased
27 excitation in unipolar depressive states is caused by diminished dendritic branches and decreased
28 density of AMPA and NMDA receptors or a decrease in glutamate released by presynaptic
29 neurons. All bipolar states result from heightened neural sensitivity due to altered sodium,
30 calcium, or potassium channel conductance. Our formal model of mood disorders is consistent
31 with fMRI studies, genetic research, as well as preclinical and clinical studies.

32 **Introduction**

33 Current psychiatric diagnoses, including diagnoses of mood disorders, are based on criteria
34 established by expert consensus rather than recognized pathophysiologies [1-2]. As a result, the
35 same diagnosis can be used for conditions which differ in symptomatology, frequency, duration,
36 and level of disability while different diagnoses may share similar symptomatology. Since
37 medications often work as neuromodulators, abnormality of neuromodulation has been the
38 prevailing hypothesis of psychopathology [3]. Researchers have increasingly questioned its
39 validity [4-7].

40 This lack of understanding of pathophysiology leads to heterogeneity in defined patient
41 populations, causing confusion in selecting subjects for research studies and in selecting effective
42 treatments for individual patients and leading to a failure of innovative treatments [8,9]. As a
43 result, a low percentage of patients diagnosed with major depression responded to their initial
44 and subsequent treatments according to one often quoted multicenter study [10].

45 We are proposing a formal model of mood disorders based upon dynamical systems interaction
46 as an alternative to the neuromodulator theory. A recent assessment of existing formal models
47 of mood disorders by Nunes proposed that an effective dynamical model must satisfy three
48 validity criteria: face, predictive and construct validity. A valid model should be able to identify
49 the target symptoms, predict the onset and transitions between symptom states and provide a
50 plausible mechanism for mood states and transitions [11]. We suggest that our model satisfies
51 these three criteria.

52 Over the past two decades significant progress has been made in understanding the function
53 and interactions of brain centers and in the application of neural network theory, matrix
54 connectivity and information theory to brain function. These mathematical formulations offer a
55 foundation for understanding the interactions of brain centers and their interconnections which
56 can be used to identify the activity of neural circuits causing mood disorders [12-18]. Using
57 network theory, we can conceptualize the vast complexity of the brain as an array of nodes
58 connected by large bundles of myelinated tracts or edges. Nodes with complementary functions
59 are connected into larger networks in a hierarchical manner with each later node

60 refining the output of the prior. As will be explained in greater detail in the methods section, we
61 conclude that the weight of evidence favors the hypothesis that mood disorder symptoms largely
62 reflect the functioning of the central executive network (CEN), the salience network (SN), and the
63 default mode network (DMN) [19-21].

64 The CEN, also called the frontoparietal network, is composed of the dorsolateral prefrontal cortex
65 and the posterior parietal cortex. It is responsible for higher reasoning, problem solving, selective
66 focusing, and choice of alternative actions based on an assessment of likely outcome. It also
67 suppresses the immediate expression of more primitive impulses [22]. A loss of CEN leads to a
68 loss of focus and reasoning and greater impulsivity [23,24].

69 The exact constituents of SN differ among researchers, but all agree that the primary hubs are
70 the anterior insula and the anterior cingulate cortex which relate to the amygdala and
71 hippocampus in association with the cortico-striato-thalamo-cortical circuit (CSTC) [25,26].

72 The SN is responsible for identifying an object of interest, assessing its value (attractive or
73 aversive) and selecting an immediate response to salient stimuli. It may also through its
74 interconnections be involved in self-awareness, communication, the integration of internal and
75 external sensation, and may activate either the CEN or the DMN. The CEN is, therefore,
76 dependent on the SN for its function [27-28]. Depression of SN-CEN circuit function leads to a
77 muted CEN response to input which may include indifference [29]. Extreme SN activity leads to
78 the characteristic symptoms of mania: hyperkinetic movements, euphoria, promiscuity, and
79 reckless risk taking- based on a summary by Cotovio et.al. who reported hyperactivity of the ACC,
80 amygdala, and basal ganglia which are components of SN-CSTC [30].

81 The default mode network (DMN) comprises the medial prefrontal cortex, posterior cingulate,
82 precuneus and angular gyrus [32]. It is so named because it is active when the CEN and SN are
83 inactive and is involved in rumination, introspection, self-reference, and daydreaming, while
84 DMN hyperactivity causes depressive brooding as well as psychosis in depression, mania, and
85 schizophrenia [33-35].

86 Genetic studies of bipolar disorder consistently identify alleles of ANK3, CACNA1C, and KCNB1
87 [36-42]. CACNA1C and KCNB1 are components of calcium and potassium channels, respectively.
88 [39-42]. ANK3 controls the density and correct placement of sodium, potassium and calcium ion
89 channels at the axon hillock, Nodes of Ranvier and apical dendrites [42-45,45,47]. Although these
90 alleles are present in only a small percentage of subjects with bipolar disorder, they nevertheless
91 suggest a pathophysiology that may result from small effects of multiple other alleles affecting
92 ion conduction. Ion conduction underlies neural sensitivity to excitation and in bipolar disorder
93 causes a high sensitivity to neural input [36,37,45-50].

94 There has been no allele consistently identified for depression [51]. However, human and animal
95 studies have shown increased dendritic sprouting and increased dendritic volume in both
96 depressed human subjects and animals treated with antidepressants, leading to the hypothesis
97 that depression results from decreased postsynaptic density of AMPA or NMDA receptors [52-
98 58].

99 To our knowledge this paper is a unique attempt to present a formal model of mood disorders
100 based on the triple circuit model and grounded in neurophysiology and genetics. Starting with a
101 simple model of single neuron dynamics, our model is consistent with fMRI studies of brain center

102 activity and connectivity, the effects of gene variants on ion channels, as well as preclinical and
103 clinical research.

104 **Method**

105 In the method section, we identify and justify the underlying assumptions of the formal model by
106 providing their grounding in neurophysiology, fMRI studies and in clinical observation. These
107 assumptions are:

- 108 1. Mood disorders are disorders of neural circuits.
- 109 2. Based on current research the most likely circuits are the CEN, SN-CSTC (SN combined
110 with nodes of the cortico-striatal thalamic circuit) and DMN.
- 111 3. The activity of each network is an average of network frequencies over prolonged periods
112 (weeks or months).
- 113 4. Since these are recurrent circuits the average activity of the circuit can be modeled on the
114 dynamics of a single neuron which is a component of the circuit.
- 115 5. The key variables of neural function are the strength of inputs, and the neuron's
116 sensitivity to inputs, which is determined by sodium, potassium, and calcium channel
117 conductance.
- 118 6. Ion channel conductance is determined by genetics or epigenetics.
- 119 7. Mood states are not attributable to a specific node but arise from the combined
120 interaction of individual nodes tied to their circuits and the interactions of those circuits.
- 121 8. The symptoms of mood disorders are caused by dysfunction within networks and
122 between interacting networks.

- 123 9. Depressive episodes are due to hypofunction of the CEN and SN-CSTC and manic episodes
124 are due to excessive activity of SN-CSTC and hypofunction of the CEN.
- 125 10. Bipolar disorder states are due to channelopathy.
- 126 11. The interactions of the networks are best quantified by using the nonlinear dynamics of
127 neuron firing rates.

128 **Review of fMRI brain center activity in mood disorder states**

129 fMRI records activity of specific brain centers which are the major nodes of neural networks, and
130 coincidence of nodal activity is a marker for the connectivity of their neural networks.

131 Patterns of activity of key brain centers in depression and bipolar mood states were determined
132 by reviewing fMRI studies of mood disorders by searching Pub Med and Google Scholar. For
133 depression, we used only studies of currently depressed subjects. For bipolar disorder we used
134 studies that clearly indicated current depression or mania and attempted to determine if the
135 subjects were medicated. We also searched for studies of fMRI activity of the centers which are
136 key to mood disorders: ventrolateral prefrontal cortex (VLPFC), dorsolateral prefrontal cortex
137 (DLPC), medial prefrontal cortex (MPFC), anterior insula (AI), anterior cingulate cortex (ACC),
138 amygdala, thalamus, hippocampus, and striatum, which will be reviewed below.

139 Systematic review of two decades of fMRI depression studies reveals inconsistent findings due
140 to small sample size, heterogeneity of patient samples, medication, differences in protocol e.g.,
141 resting state versus task oriented, and technical difficulties such as noise to signal ratio. The
142 preponderance of evidence supports a loss of function of the prefrontal cortex, as well as
143 decreased activity or connectivity of the AI, ACC, ventral striatum, basal ganglia, and medial

144 thalamus [59-67]. In depressed subjects the amygdala may be hyperactive in tasks which evoke
145 negative emotion [68-69].

146 fMRI studies of mania are contradictory due to the impracticality of obtaining compliance from
147 unmedicated acutely manic subjects. fMRI studies show hyperactivity of the amygdala, basal
148 ganglia, and ACC based on a summary of studies using varied methodologies by Cotovio, as well
149 as increased ACC and caudate activity in a small study by PET scan [53-54]. Studies of functional
150 connectivity in mania, while generally agreeing with a decreased VLPFC, and increased amygdala
151 activity, as well as decreased suppression of amygdala hyperactivity by the VLPFC, nevertheless,
152 do not require actively symptomatic or unmedicated subjects, often do not specify bipolar state,
153 use small numbers of subjects, and use highly divergent methodologies [70-74].

154 In identifying candidate networks, we used a simplifying assumption that in a recurrent network
155 the dominant node, with greatest effective connectivity, should set the prevailing frequency over
156 prolonged time periods. We found that the crucial nodes for mood disorders most frequently
157 identified by fMRI studies were constituent nodes of the CEN, DMN and SN combined with the
158 CSTC [59-76]. Also, connectivity studies confirmed the presence or absence of an inter-
159 connection between the key nodes of the CEN, DMN and SN-CSTC (fig. 1) and supports the
160 conclusion that abnormalities in the function of one circuit leads to abnormal function of any
161 circuit with which it interacts [59-67, 74-79]. Therefore, the symptoms of mood disorders arise
162 from the disordered function of one or more networks and their interactions. The fMRI studies
163 indicate that depressive symptoms result from low activity of key nodes of the CEN and SN and
164 increased activity of the DMN [77-79]. In the depressive state the amygdala may be hyperactive

165 but has decreased functional connectivity with other nodes of the SN-CSTC [80, 81]. The manic
166 state results from an unrestrained SN-CSTC with subdued CEN [30, 31].

167 In our model of bipolar disorder, we assume a channelopathy affecting SN which causes an
168 excessive sensitivity to change in SN recurrent activity [43-50].

169

170 **Fig 1. Diagram of triple circuit dynamics**

171 A schematic model showing the interconnections of the three network model.

172

173 **Network Model**

174 Differential equations can be used to model the dynamics of the networks with greater clarity
175 and predictive power because recurrent and internetwork output evolve over time. The network
176 is modeled as a weighted directed graph, with weightings representing the strength of the
177 connections within and between the individual nodes in the network. These weightings appear
178 in the governing differential equations in the form of the connectivity matrix [13].

179 Network activity is specified as a relative firing rate. How information is encoded and transmitted
180 by neurons is under active investigation [82]. However, for our purposes we are more interested
181 in whole circuit activity as measured by the metabolic needs of the constituent nodes and
182 dependent on the percentage of activated neurons and their firing rates, as captured by fMRI.
183 This activity would be averaged over periods of weeks or months, typical of episodes of mood
184 disorders.

185 We use an equation for single neuron dynamics [35,36] to represent the activity of the entire
186 circuit, simplifying circuit dynamics by making the network frequency dependent on only two
187 parameters- the average neuron's weighting (W), given by the adjacency matrix, and sensitivity
188 to stimulation (σ) [35,36] (fig. 1). In our simple model, all networks have the same σ for euthymia
189 and unipolar depression, however, for all bipolar states SN has a greater σ .

190 Positive and negative weightings indicate excitatory or inhibitory connections. We use the
191 convention that W_{ij} denotes the influence that network i has on network j . For example, W_{SE}
192 denotes the influence of SN on CEN. The assigned weighting of intra-network stimulation (e.g.,
193 W_{SE}) and inter-network stimulation (e.g., W_{ss}) is the sum of all excitatory and inhibitory
194 weightings of feedforward and feedback connections.

195 We use weightings to produce levels of network activation that model the fMRI results of
196 network nodes associated with the specified mood disorder. In our model all network variables
197 must be relative since the actual values for average frequency, weightings, and slope of activation
198 in mood states are not known.

199 For all unipolar mood states all networks are at homeostatic equilibrium: If their firing rates are
200 altered, they will shortly return to their fixed firing rate. However, for all bipolar states we assign
201 less stable fixed points to produce the rapid and dramatic fluctuations in mood characteristic of
202 bipolar disorder. To create relatively unstable fixed points, we increase the σ of SN. This implies
203 higher sodium or calcium conductance or lower potassium conductance in all bipolar states.

204 The matrix W gives the weightings of inter and recurrent stimulation of the networks and follows
205 the conclusions regarding the interactions of the triple circuits. We assigned a relatively lower

206 recurrent weighting to the CEN, making the CEN more vulnerable to changes in inter-network
207 excitation. Other rules for network interconnections are: SN is the primary driver, it can increase
208 or decrease SN-CEN and SN-DMN; CEN weightings are only inhibitory; it can decrease SN and
209 decrease DMN; DMN is passive, it is acted upon by SN or CEN. SN, through its dominant AI node,
210 can turn on or off the CEN and DMN even when SN activity is high [27,28].

211 **Formulation of network equations**

212 In the model, the strength of influence of unit i on unit j will be represented by a scalar called
213 the *weighting*, which will be denoted w_{ij} . For example, the strength of influence of the salience
214 network on the central executive network is denoted w_{SE} , and is represented in Figure 1 as the
215 arrow from S to E . The governing equation of such a firing rate network is given by equation
216 7.10 of [12]:

$$217 \quad \tau_i \frac{dv_i}{dt} = -v_i + F((W\vec{v}) \cdot \vec{e}_i)$$

218 where:

- 219 • v_i represents the firing rate of unit i . For example, v_S denotes the firing rate of the
220 salience network;
- 221 • \vec{v} is a vector containing the firing rate of each unit, $\vec{v} = (v_S, v_E, v_D)$;
- 222 • $W = [\vec{W}_1 \ \vec{W}_2 \ \vec{W}_3]^T$ is the matrix containing the weightings of all of the connections
223 within the network, and \vec{W}_i denotes the weightings of all connections going in to node i ;
- 224 • τ_i is a time constant;

- 225 • e_i is the i^{th} standard basis vector;
- 226 • F is the “activation function” of the neurons, representing how the firing rate of a
- 227 neural unit changes as a function of its input current.

228 We use the sigmoidal activation function

$$229 \quad F(I) = \frac{v_{max}}{1 + \exp(-\sigma I + I_{th})} + v_{min}.$$

230 In this expression, I is the total input current to the neural unit, v_{max} is the maximum firing rate
231 of the neural unit, v_{min} the minimum possible firing rate - which we take to be small but
232 nonzero - I_{th} is the activation threshold, and σ is a parameter which controls the steepness of
233 the activation curve. Biologically, the parameter σ represents the overall sensitivity of a neural
234 unit to input current. In a biological neuron, sensitivity is determined by a range of factors,
235 including ion channel density and synaptic sensitivity - in our model, σ represents an
236 amalgamation of all such factors. A larger value of σ corresponds to a more sensitive neural
237 unit, and vice versa. In some texts, see for example [12], the constants are taken to be v_{max}
238 = 100Hz, $I_{th} = 50\text{nA}$, $\sigma = 17.5$, and $\tau = 5\text{ms}$. We choose to scale our parameters in such a
239 way that emphasizes qualitative behavior of the network, rather than focusing on specific
240 quantitative relationships.

241 In this scaling, v_i represents the firing rate of unit i , represented as a fraction of its maximum
242 possible firing rate. For example, if $v_i = 0.6$, this means that unit i is firing at 60% of its
243 maximum possible firing rate. Finally, for simplicity, we take all the time constants to be equal

244 and set them to $\tau_1 = \tau_2 = \tau_3 = 5$. Therefore, the parameters that we manipulate in this model
245 are the weightings between neurons, W , and the activation sensitivity σ .

246

247 Results

248 For the euthymic state, σ is set at 2.2 which represents moderate slope of activation to
249 depolarizing current based upon the density of sodium, calcium and potassium channels at the
250 axon hillock and axon terminals of all three networks (CEN, SN, DMN). In the euthymic state
251 recurrent CEN weighting (W_{EE} , 0.9) is far smaller than recurrent SN weighting (W_{SS} , 2.0) causing
252 CEN function to be highly dependent on SN input from AI. The euthymic state is homeostatic with
253 stable intra and inter network activity of the three networks which all function at midrange
254 activity. The connectivity matrix used in the euthymic state is given by: W_{SS} 2.0, W_{SE} 0.8, W_{SD} 0.6,
255 W_{ES} -3.5, W_{EE} 0.9, W_{ED} -0.5, W_{DS} 0, W_{DE} 0, W_{DD} 1.5. The resulting behavior of the three networks
256 is shown in Figure 2.

257

258

Fig 2. Euthymic

259 In the euthymic state, all three networks tend towards a stable fixed point at an intermediate
260 firing rate, corresponding to a healthy homeostatic state.

261

262 For unipolar depression, σ remains at 2.2. The unipolar depressive syndrome is caused by a
263 decrease in the SN recurrent stimulation by 25%. Although CEN network recurrent weighting

264 remains constant, its activity is greatly reduced by decreased SN input. Decreased CEN activity
265 leads to heightened DMN activity of 13%. The connectivity matrix for this state is given by W_{SS}
266 1.5, W_{SE} 0.8, W_{SD} 0.6, W_{ES} -3.5, W_{EE} 0.9, W_{ED} -0.5, W_{DS} 0, W_{DE} 0, W_{DD} 1.7. The
267 network dynamics of the unipolar state are shown in Figure 3.

268 **Fig 3. Unipolar depressed**

269 In unipolar depression, the salience network and the central executive network are both
270 operating at an extremely low activity level, while the default mode network maintains an
271 elevated level of activity.

272

273 For bipolar disorder, the SN σ is increased to 2.5 in all bipolar states, 13.6% higher than the SN σ
274 for euthymia and unipolar depression, while CEN σ and DMN σ remain at 2.2. (fig. 4-5) This small
275 increase bipolar SN σ causes extreme responses in SN activation due to small changes in SN
276 recurrent excitation. The bipolar euthymic state requires a 71% increase in inhibition of CEN-SN
277 and decreased SN-CEN excitation of 25%. The connectivity matrix used to generate this state is:
278 W_{SS} 2, W_{SE} 0.6, W_{SD} 0.6, W_{ES} -0.6, W_{EE} 0.9, W_{ED} -0.5, W_{DS} 0, W_{DE} 0, W_{DD} 1.5. The network dynamics
279 are illustrated in Figure 4.

280

281 **Fig 4. Bipolar euthymic**

282 The euthymic bipolar state is indistinguishable from true euthymic, with similar activation of each of the
283 three networks. Bipolar depression is caused by a minor change in the network weightings: The activity
284 of the salience and executive networks collapse, while the default mode network maintains high activity.
285 The sensitivity to network parameters is caused by the increased sensitivity σ of the salience network.

286

287 Bipolar depression results from a 10% reduction of SN recurrent excitation. The connectivity
288 matrix is: $W_{SS} 1.8$, $W_{SE} 0.6$, $W_{SD} 0.6$, $W_{ES} -0.6$, $W_{EE} 0.9$, $W_{ED} -0.2$, $W_{DS} 0$, $W_{DE} 0$, $W_{DD} 1.5$. The
289 network dynamics are shown in figure 5.

290

291

Fig. 5. Bipolar Depressed.

292 Bipolar depression is caused by a minor change in the network weightings: The activity of the salience
293 and executive networks collapse, while the default mode network maintains high activity. The sensitivity
294 to network parameters is caused by the increased sensitivity σ of the salience network.

295

296 Bipolar mania is caused by reduction of SN-CEN excitation by 50% and a corresponding increased
297 SN-DMN excitation of 33%. The connectivity matrix is: $W_{SS} 2.0$, $W_{SE} 0.2$, $W_{SD} 0.4$, $W_{ES} -0.6$, W_{EE}
298 0.9 , $W_{ED} -0.5$, $W_{DS} 0$, $W_{DE} 0$, $W_{DD} 1.5$. The network dynamics are shown in figure 6.

299

300

301

Fig 6. Bipolar manic

302 A slight change of the network weightings causes the bipolar-euthymic state to enter a manic
303 state, in which the executive network is depressed, and the salience and default mode networks
304 have extremely heightened activity.

305

306 Therefore, our model attributes both unipolar and bipolar depression to an initial loss of
307 recurrent excitation of the SN and mania to a shift in SN excitation from CEN to DMN. Although
308 not illustrated, excessive DMN activity may arise from increased W_{DD} , increased W_{SD} or decreased
309 W_{ED} (through decreased CEN-DMN inhibition) and produces psychotic symptoms [34,35].

310 Discussion

311 We have presented what we believe is a unique formal model of mood disorders arising from the
312 dynamics of coupled neural circuits that serves as an alternative paradigm to neuromodulation
313 theory. It grounds mood states in a model which is consistent with what is known of
314 neurophysiology and genetics and its assumptions are clear and capable of validation. It presents
315 mood disorders as a group of symptoms arising from fluctuations of system parameters, much
316 as the weather. While other formal models of the dynamics of mood disorders have been
317 proposed, ours is unique because of its strong grounding in pathophysiology [11].

318 We demonstrate how intra-network recurrent excitation or inhibition can be based on the
319 dynamics of neural circuits by using nonlinear dynamics and show how the resulting intra-

320 network interactions of the CEN, SN-CSTC, and DMN networks lead to the pathologic circuit
321 activity which underlies the symptom clusters of mood disorders.

322 The extreme complexity of brain function has presented a Gordian Knot which has been
323 impossible to resolve. We have presented a radical simplification, comprising three circuits, their
324 weightings of intrasynaptic strength and their neural sensitivity based on ion channel function.
325 We model intra-circuit dynamics on recurrent networks: The entire network shares the dynamics
326 of a single constituent neuron with all elements of a circuit conforming to the dynamics of a single
327 nodal component. By simplifying an enormously complex problem we may have constructed a
328 useful heuristic model for further research.

329 Any simplification opens itself to the criticism that it is overly simplistic and ignores important
330 exceptions. In its defense we point out the extremely contradictory conclusions of decades of
331 studies based upon small samples, different inclusion and exclusion criteria for subjects, the
332 marked ambiguity of criteria for diagnoses, and the vagaries and artifacts of the emerging
333 technologies of fMRI and genetic testing. With all the noise it is difficult to isolate a signal.

334 In constructing our model, we attempted to find the most replicated of conflicting results or a
335 consensus opinion. Ultimately a researcher reviewing the studies must employ Bayesian
336 probability as a tool of analysis, factoring one's prior assumptions when weighing the likelihood
337 of given test results- a technique which all seasoned clinicians employ in their daily practice.

338 Ultimately the question is, does this model work? Are its underlying assumptions provable? Does
339 it lead to research that discovers previously unknown truths? Does it lead to new treatments?
340 Does it lead to better ways of constructing studies?

341 We propose that the underlying cause of both unipolar depression and bipolar disorder lies
342 within SN and that the underlying pathophysiology of bipolar disorder is a heightened sensitivity
343 of the SN resulting from abnormal conductance of sodium, calcium and/or potassium channels
344 due to genetic or epigenetic influences [35-50]. Applying the neural circuit model, both the
345 rapidity and frequency of mood changes in the bipolar states result from unstable fixed points
346 created by the heightened sensitivity of the SN.

347 Our formal model explains the mechanism of action of most bipolar medications- lithium, sodium
348 valproate and atypicals - as sodium channel blockers [83-87]. It predicts that channelopathies
349 and an abnormally high σ will be found in the key nodes of the SN-amygdala in

350 cadaver studies of Bipolar I subjects. In our model excessive excitation of the DMN results in
351 psychotic symptoms and explains the shared genetics of schizophrenia and bipolar disorder to
352 alleles which cause excessive excitation of the DMN [34-35].

353 Transcranial magnetic stimulation (TMS) may ultimately prove to offer a more specific treatment
354 for mood disorders. TMS treatment of depression induces a current between the dorsolateral
355 prefrontal cortex and regions of SN [88-89]. TMS with deep cranial penetration may be more
356 effective by reaching the deeper brain structures of the SN [90-92].

357 An implication of the theory is the importance of selecting subjects with homologous phenotypes
358 for clinical treatment studies. The original Feigner criteria emphasized the episodic nature of
359 major depression and bipolar disorder have been considerably broadened allowing for marked
360 heterogeneity among research subjects ([1,2,93,94]. Homogeneity in research studies is better
361 insured by similar symptomatology in unmedicated subjects rather than similar but amorphous

362 diagnoses. Treatment studies should also use subjects homologous for symptoms as well as
363 chronicity and general level of function. For example, in the STAR D study
364 there was a considerably better response to antidepressants in the subset of subjects with a work
365 history [95].

366 fMRI is currently the most effective means of identifying network pathology. However, since
367 abnormalities of circuit activation are state dependent and state specific, fMRI studies of all
368 bipolar subjects, regardless of state, are misleading as are studies of depressed patients
369 irrespective of symptom profile and medication usage. Ideally, fMRI studies would compare
370 imaging during and after episodes in large groups of symptomatically similar subjects to identify
371 state driven abnormalities. Treatment studies of mood disorders should use unmedicated
372 subjects with similar pretreatment fMRI and standardized fMRI protocols.

373 The dynamic model explains the differing response of unipolar and bipolar depressives to the
374 increased feedforward excitation caused by antidepressants: The increased SN sensitivity of
375 bipolar patients to antidepressant causes a manic response.

376 In conclusion our formal model fulfills the requirements given by Nunes et.al, outlining the
377 necessary elements of a useful model of mood disorders: face, predictive and construct validity
378 [11]. Its assumptions are testable, and its conclusions may lead to improvements in diagnosis,
379 and treatment and suggest novel directions for future research.

380

381 **Author Contributions**

382 Alan Lawrence Rubin performed the research, identified the neural circuit model and the
383 mathematical model used, and wrote the paper.

384 Mark Walth completed the mathematical analysis and designed the graphs.

385

386 **Acknowledgments**

387 None

388 **Conflict of interest**

389 The authors attest that there are no financial conflicts of interest.

390 **References**

391 1. Goodkind M, Eickhoff SB, Oathes DJ, Jiang Y, Chang A, Jones-Hagata LB, Ortea BN, Zaiko YV,

392 Roach EL, Korgaonkar MS, Grieve SM. Identification of a common neurobiological substrate for mental

393 illness. *JAMA Psychiatry* 72: 305–315.

394 2. Phillips ML, Kendler KS. Three important considerations for studies examining pathophysiological

395 pathways in psychiatric illness: in-depth phenotyping, biological assessment, and causal inferences. *JAMA*

396 *psychiatry*. 2021 Jul 1;78(7):697-8.

397 3. Liu B, Liu J, Wang M, Zhang Y, Li L. From serotonin to neuroplasticity: evolution of theories for major

398 depressive disorder. *Frontiers in cellular neuroscience*. 2017 Sep 28;11:305.

399 4. Moncrieff J, Cooper RE, Stockmann T, Amendola S, Hengartner MP, Horowitz MA. The serotonin theory

400 of depression: a systematic umbrella review of the evidence. *Molecular psychiatry*. 2022 Jul 20:1-4.

401 5. Kennis Ruhé HG, Mason NS, Schene AH. Mood is indirectly related to serotonin, norepinephrine and

402 dopamine levels in humans: a meta-analysis of monoamine depletion studies. *Molecular psychiatry*. 2007

- 403 Apr;12(4):331-59.
- 404 6. Kennis M, Gerritsen L, van Dalen M, Williams A, Cuijpers P, Bockting C. Prospective biomarkers of major
405 depressive disorder: a systematic review and meta-analysis. *Molecular psychiatry*. 2020 Feb;25(2):321-
406 38.
- 407 7. Anticevic, A. Krystal, JH, Murray, JD: Meeting emerging challenges and opportunities in psychiatry
408 through computational neuroscience. *Computational Psychiatry* ed by Anticevic MA, Murray JD,
409 Academic Press, Elsevier 2018; xiii-xxxi5.
- 410 8. O'Brien PL, Thomas CP, Hodgkin D, Levit KR, Mark TL. The diminished pipeline for medications to treat
411 mental health and substance use disorders. *Psychiatric Services*. 2014 Dec 1;65(12):1433-8.
- 412 9. Insel TR, Wang PS. The STAR* D trial: revealing the need for better treatments. *Psychiatric services*.
413 2009 Nov;60(11):1466-7.
- 414 10. Rush AJ. Limitations in efficacy of antidepressant monotherapy. *Journal of Clinical Psychiatry*. 2007
415 1;68(B):8.
- 416 11. Nunes A, Singh S, Allman J, Becker S, Ortiz A, Trappenberg T, Alda M. A critical evaluation of dynamical
417 systems models of bipolar disorder. *Translational Psychiatry*. 2022 Sep 28;12(1):416.
- 418 12. Dayan P, Abbott, LF: *Theoretical Neuroscience: Computational and Mathematical Modeling of Neural*
419 *Systems*. 2001; MIT Press.
- 420 13. Miller, P: *Introductory Course in Computational Neuroscience*. 2018; MIT Press.
- 421 14. Sporns O. *Networks of the Brain*. MIT press; 2016 Feb 12.

- 422 15. Cannon J, Miller P: Stable control of firing rate mean and variance by dual homeostatic mechanisms.
423 Journal of Mathematical Neuroscience 2017; 7:1:1-38
- 424 16. Avena-Koenigsberger A, Misisic B, Sporns O. Communication dynamics in complex brain networks.
425 Nature reviews neuroscience. 2018 Jan;19(1):17-33.
- 426 17. Bullmore E, Sporns O. Complex brain networks: graph theoretical analysis of structural and functional
427 systems. Nature reviews neuroscience. 2009 Mar;10(3):186-98.
- 428 18. Sporns O. Contributions and challenges for network models in cognitive neuroscience. Nature
429 neuroscience. 2014 May;17(5):652-60.
- 430 19. Bressler SL, Menon V. Large-scale brain networks in cognition: emerging methods and principles.
431 Trends in cognitive sciences. 2010 Jun 1;14(6):277-90.
- 432 20. Menon V. Large-scale brain networks and psychopathology: a unifying triple network model. Trends
433 in cognitive sciences. 2011 Oct 1;15(10):483-506.
- 434 21. Chen, A. C., Oathes, D. J., Chang, C., Bradley, T., Zhou, Z. W., Williams, L. M., ... & Etkin, A. (2013). Causal
435 interactions between fronto-parietal central executive and default-mode networks in
436 humans. Proceedings of the National Academy of Sciences, 110(49), 19944-19949.
- 437 22. Ridderinkhof KR, Van Den Wildenberg WP, Segalowitz SJ, Carter CS. Neurocognitive mechanisms of
438 cognitive control: the role of prefrontal cortex in action selection, response inhibition, performance
439 monitoring, and reward-based learning. Brain and cognition. 2004 Nov 1;56(2):129-40.
- 440 23. Daigle KM, Pietrzykowski MO, Waters AB, Swenson LP, Gansler DA. Central executive network and

- 441 executive function in patients with Alzheimer’s disease and healthy individuals: meta-analysis of structural
442 and functional MRI. *The Journal of Neuropsychiatry and Clinical Neurosciences*. 2022 Jul;34(3):204-13.
- 443 24. Ryan NP, Catroppa C, Hughes N, Painter FL, Hearps S, Beauchamp MH, Anderson VA. Executive
444 function mediates the prospective association between neurostructural differences within the central
445 executive network and anti-social behavior after childhood traumatic brain injury. *Journal of child
446 psychology and psychiatry*. 2021 Sep;62(9):1150-61.
- 447 25. Menon V. Salience network. *Brain mapping: an encyclopedic reference*. Academic Press: Cambridge,
448 MA, USA, Elsevier: Amsterdam, The Netherlands. 2015;2:597-611.
- 449 26. Peters SK, Dunlop K, Downar J. Cortico-striatal-thalamic loop circuits of the salience network: a
450 central pathway in psychiatric disease and treatment. *Frontiers in systems neuroscience*. 2016 Dec
451 27; 10:104.
- 452 27. Sridharan D, Levitin DJ, Menon V. A critical role for the right fronto-insular cortex in switching between
453 central-executive and default-mode networks. *Proceedings of the National Academy of Sciences*. 2008
454 Aug 26;105(34):12569-74.
- 455 28. Goulden, N., Khusnulina, A., Davis, N. J., Bracewell, R. M., Bokde, A. L., McNulty, J. P., & Mullins, P. G.
456 (2014). The salience network is responsible for switching between the default mode network and the
457 central executive network: replication from DCM. *Neuroimage*, 99, 180-190.
- 458 29. Chand GB, Wu J, Hajjar I, Qiu D. Interactions of the salience network and its subsystems with the
459 default-mode and the central-executive networks in normal aging and mild cognitive impairment. *Brain
460 connectivity*. 2017 Sep 1;7(7):401-12.

- 461 30. Cotovio C, Oliveira-Maia AJ: Functional Neuratomy of Mania. *Translational Psychiatry* 2022; 12:29
- 462 31. Blumberg, HP, Stern E, Martinez D, Ricketts S, et al: Increased anterior cingulate and caudate activity
463 in bipolar mania. *Biol Psychiatry* 2000; 48:1045-1052 16.
- 464 32. Horn A, Ostwald D, Reisert M, Blankenburg F. The structural–functional connectome and the default
465 mode network of the human brain. *Neuroimage*. 2014 Nov 15;102:142-51.
- 466 33. Berman MG, Peltier S, Nee DE, Kross E, Deldin PJ, Jonides J. Depression, rumination and the default
467 network. *Social cognitive and affective neuroscience*. 2011 Oct 1;6(5):548-55.
- 468 34. Meda SA, Ruaño G, Windemuth A, O’Neil K, Berwise C, Dunn SM, Boccaccio LE, Narayanan B,
469 Kocherla M, Sprooten E, Keshavan MS. Multivariate analysis reveals genetic associations of the resting
470 default mode network in psychotic bipolar disorder and schizophrenia. *Proceedings of the National*
471 *Academy of Sciences*. 2014 May 13;111(19):E2066-75.
- 472 35. Peeters, S. C., van de Ven, V., Gronenschild, E. H. M., Patel, A. X., Habets, P., Goebel, R., ... & Genetic
473 Risk and Outcome of Psychosis (GROUP). (2015). Default mode network connectivity as a function of
474 familial and environmental risk for psychotic disorder. *PloS one*, 10(3), e0120030.
- 475 36. Roby Y. ANK3 gene polymorphisms and bipolar disorder: a meta-analysis. *Psychiatr Genet*. 2017
476 Dec;27(6):225-235.
- 477 37. Leussis MP, Madison JM, Petryshen TL. Ankyrin 3: genetic association with bipolar disorder and
478 relevance to disease pathophysiology. *Biology of mood & anxiety disorders*. 2012 Dec;2(1):1-3.
- 479 38. Leussis MP, Berry-Scott EM Saito M, Jhuang H et al: The ANK3 bipolar disorder gene regulates

- 480 psychiatric-related behaviors that are modulated by lithium and stress. *Biopsych* 2013 April; 73:7 683-
481 690.
- 482 39.Ferreira MA, O'Donovan MC, Meng YA, Jones IR, Ruderfer DM, Jones L, Fan J, Kirov G, Perlis RH, Green
483 EK, Smoller JW. Collaborative genome-wide association analysis supports a role for ANK3 and CACNA1C
484 in bipolar disorder. *Nature genetics*. 2008 Sep;40(9):1056-8.
- 485 40.Fiorentino A, O'Brien NL, Locke DP, McQuillin A, Jarram A, Anjorin A, Kandaswamy R, Curtis D, Blizard
486 RA, Gurling HM. Analysis of ANK3 and CACNA1C variants identified in bipolar disorder whole genome
487 sequence data. *Bipolar disorders*. 2014 Sep;16(6):583-91.
- 488 41.Li M, Li T, Xiao X, Chen J, Hu Z, Fang Y. Phenotypes, mechanisms and therapeutics: insights from
489 bipolar disorder GWAS findings. *Molecular Psychiatry*. 2022 Jul;27(7):2927-39.
- 490 42.Judy JT, Seifuddin F, Pirooznia M, Mahon PB, Bipolar Genome Study Consortium, Jancic D, Goes FS,
491 Schulze T, Cichon S, Noethen M, Rietschel M. Converging evidence for epistasis between ANK3 and
492 potassium channel gene KCNQ2 in bipolar disorder. *Frontiers in genetics*. 2013 May 17; 4:87.
- 493 43. Platkiewicz J, Brette R. A threshold equation for action potential initiation. *PLoS computational biology*.
494 2010 Jul 8;6(7):e1000850.
- 495 44.Barry J, Gu Y, Jukkola P, O'Neill B, Gu H, Mohler PJ, Rajamani KT, Gu C. Ankyrin-G directly binds to
496 kinesin-1 to transport voltage-gated Na⁺ channels into axons. *Developmental cell*. 2014 Jan 27;28(2):117-
497 31.
- 498 45.Pan Z, Kao T, Horvath Z, Lemos J, Sul JY, Cranstoun SD, Bennett V, Scherer SS, Cooper EC. A common
499 ankyrin-G-based mechanism retains KCNQ and NaV channels at electrically active domains of the axon.
500 *Journal of neuroscience*. 2006 Mar 8;26(10):2599-613.

- 501 46. Zeberg H, Blomberg C, Århem P. Ion channel density regulates switches between regular and fast
502 spiking in soma but not in axons. *PLoS computational biology*. 2010 Apr 22;6(4):e1000753.
- 503 47. Motipally SI, Allen KM, Williamson DK, Marsat G. Differences in sodium channel densities in the apical
504 dendrites of pyramidal cells of the electrosensory lateral line lobe. *Frontiers in Neural Circuits*. 2019 Jun
505 4;13:41.
- 506 48. Gunay c, Edgerton JR, Jaeger D: Channel density distributions explain spiking variability in the globus
507 pallidus: a combined physiology and computer simulation database approach. *Journal of Neuroscience*:
508 2008; 28 (30)7476-7491.
- 509 49. Arhem P, Klement, G, Blomberg C: Channel density regulation of firing patterns in a cortical neuron
510 model. *Biophysical Journal*: 2006; 90:12 4392-440461.
- 511 50. Huang M, Volgushev M, Wolf F. A small fraction of strongly cooperative sodium channels boosts
512 neuronal encoding of high frequencies. *PLoS One*. 2012 May 29;7(5):e37629..
- 513 51. Border R, Johnson EC, Evans LM, Smolen A, Berley N, Sullivan PF, Keller MC. No support for historical
514 candidate gene or candidate gene-by-interaction hypotheses for major depression across multiple large
515 samples. *American Journal of Psychiatry*. 2019 May 1;176(5):376-87.
- 516 52 Fries GR, Saldana VA, Finnstein J, Rein T. Molecular pathways of major depressive disorder converge
517 on the synapse. *Molecular Psychiatry*. 2023 Jan;28(1):284-97.
- 518 53. Seo MK, Lee CH, Cho HY, Lee JG, Lee BJ, Kim JE, Seol W, Kim YH, Park SW. Effects of antidepressant
519 drugs on synaptic protein levels and dendritic outgrowth in hippocampal neuronal cultures.
520 *Neuropharmacology*. 2014 Apr 1;79:222-33.

- 521 54. Castrén E, Hen R. Neuronal plasticity and antidepressant actions. *Trends Neurosci.* 2013
522 May;36(5):259-67. doi: 10.1016/j.tins.2012.12.010. Epub 2013 Feb 1. PMID: 23380665; PMCID:
523 PMC3648595.
- 524 55. Holmes SE, Scheinost D, Finnema SJ, Naganawa M, et al: Lower synaptic density is associated with
525 depression severity and network alterations. *Translational Psychiatry* 2021; 11:511.
- 526 56. Pittenger, C, Dunma RS: Stress, depression, and neuroplasticity: a convergence of mechanisms.
527 *Neuropsychopharmacology.* 2008 Jan;33(1):88-109.
- 528 57. Kang HJ, Voleti B, Hajszan T, Rajkowska G, et al: Decreased expression of synapse-related genes and
529 loss of synapses in major depressive disorder. *Nat Med.* 2012 Sep;18(9):1413-7.
- 530 58. Licznarski P, Duman RS: Remodeling of axo-spinous synapses in the pathophysiology and treatment of
531 depression. *Neuroscience.* 2012 Oct 22; 251:33-50.
- 532 59 Drevets WC, Videen TO, Price JL, Preskorn SH, Carmichael ST, Raichle ME. A functional anatomical study
533 of unipolar depression. *Journal of Neuroscience.* 1992 Sep 1;12(9):3628-41. 2 Jul;32(4):582-595.
- 534 60. Disner SG, Beevers CG, Haigh EA, Beck AT. Neural mechanisms of the cognitive model of depression.
535 *Nature Reviews Neuroscience.* 2011 Aug;12(8):467-77.
- 536 61. Zeng, L. L., Shen, H., Liu, L., Wang, L., Li, B., Fang, P., ... & Hu, D. (2012). Identifying major depression
537 using whole-brain functional connectivity: a multivariate pattern analysis. *Brain*, 135(5), 1498-1507.
- 538 62. Pilmeyer J, Huijbers W, Lamerichs R, Jansen JF, Breeuwer M, Zinger S. Functional MRI in major
539 depressive disorder: A review of findings, limitations, and future prospects. *Journal of Neuroimaging.* 2022
540 Jul;32(4):582-95.
- 541 63. Manoliu A, Meng C, Brandl F, Doll A, Tahmasian M, Scherr M, Schwerthöffer D, Zimmer C, Förstl H,

- 542 Bäuml J, Riedl V. Insular dysfunction within the salience network is associated with severity of symptoms
543 and aberrant inter-network connectivity in major depressive disorder. *Frontiers in human neuroscience*.
544 2014 Jan 21;7:930.
- 545 64. Zheng, H., Li, F., Bo, Q., Li, X., Yao, L., Yao, Z., ... & Wu, X. (2018). The dynamic characteristics of the
546 anterior cingulate cortex in resting-state fMRI of patients with depression. *Journal of affective*
547 *disorders*, 227, 391-397.
- 548 65. Kaiser RH, Andrews-Hanna JR, Wager TD, Pizzagalli DA. Large-scale network dysfunction in major
549 depressive disorder: a meta-analysis of resting-state functional connectivity. *JAMA Psychiatry*. 2015
550 Jun;72(6):603-11.
- 551 66. Javaheripour N, Li M, Chand T, Krug A, Kircher T, Dannlowski U, Nenadić I, Hamilton JP, Sacchet MD,
552 Gotlib IH, Walter H. Altered resting-state functional connectome in major depressive disorder: a mega-
553 analysis from the PsyMRI consortium. *Translational psychiatry*. 2021 Oct 7;11(1):511.
- 554 67. Zhukovsky P, Anderson JA, Coughlan G, Mulsant BH, Cipriani A, Voineskos AN. Coordinate-based
555 network mapping of brain structure in major depressive disorder in younger and older adults: a systematic
556 review and meta-analysis. *American Journal of Psychiatry*. 2021 Dec;178(12):1119-28.
- 557 68. Peluso MA, Glahn DC, Matsuo K, Monkul ES, Najt P, Zamarripa F, Li J, Lancaster JL, Fox PT, Gao
558 JH, Soares JC. Amygdala hyperactivation in untreated depressed individuals. *Psychiatry Research:*
559 *Neuroimaging*. 2009 Aug 30;173(2):158-61.
- 560 69. Sheline YI, Barch DM, Donnelly JM, Ollinger JM, Snyder AZ, Mintun MA. Increased amygdala
561 response to masked emotional faces in depressed subjects resolves with antidepressant treatment: an
562 fMRI study. *Biological psychiatry*. 2001 Nov 1;50(9):651-8.

- 563 70. Altshuler L, Bookheimer S, Proenza MA, Townsend J, Sabb F, Firestine A, Bartzokis G, Mintz J,
564 Mazziotta J, Cohen MS. Increased amygdala activation during mania: a functional magnetic resonance
565 imaging study. *American Journal of Psychiatry*. 2005 Jun 1;162(6):1211-3.
- 566 71. Foland LC, Altshuler LL, Bookheimer SY, Eisenberger N, Townsend J, Thompson PM. Evidence for
567 deficient modulation of amygdala response by prefrontal cortex in bipolar mania. *Psychiatry Research:*
568 *Neuroimaging*. 2008 Jan 15;162(1):27-37.
- 569 72. Strakowski SM, Eliassen JC, Lamy M, Cerullo MA, Allendorfer JB, Madore M, Lee JH, Welge JA,
570 DelBello MP, Fleck DE, Adler CM. Functional magnetic resonance imaging brain activation in bipolar
571 mania: evidence for disruption of the ventrolateral prefrontal-amygdala emotional pathway. *Biological*
572 *psychiatry*. 2011 Feb 15;69(4):381-8.
- 573 73. Cerullo MA, Fleck DE, Eliassen JC, Smith MS, DelBello MP, Adler CM, Strakowski SM. A longitudinal
574 functional connectivity analysis of the amygdala in bipolar I disorder across mood states. *Bipolar*
575 *disorders*. 2012 Mar;14(2):175-84.
- 576 74 Hassel S, Almeida JR, Kerr N, Nau S, Ladouceur CD, Fissell K, Kupfer DJ, Phillips ML. Elevated striatal and
577 decreased dorsolateral prefrontal cortical activity in response to emotional stimuli in euthymic
578 bipolar disorder: no associations with psychotropic medication load. *Bipolar disorders*. 2008
579 Dec;10(8):916-27.
- 580 75. Strakowski SM, Adler CM, Almeida J, Altshuler LL, Blumberg HP, Chang KD, DelBello MP, Frangou S,
581 McIntosh A, Phillips ML, Sussman JE. The functional neuroanatomy of bipolar disorder: a consensus model.
582 *Bipolar disorders*. 2012 Jun;14(4):313-25.

- 583 76. Bi B, Che D, Bai Y. Neural network of bipolar disorder: Toward integration of neuroimaging and
584 neurocircuit-based treatment strategies. *Translational Psychiatry*. 2022 Apr 5;12(1):143.
- 585 77. Zhu X, Wang X, Xiao J, Liao J, Zhong M, Wang W, Yao S. Evidence of a dissociation pattern in resting-
586 state default mode network connectivity in first-episode, treatment-naive major depression patients.
587 *Biological psychiatry*. 2012 Apr 1;71(7):611-7.
- 588 78. Duran M, Miller C. Functional connectivity of the triple network model in major depressive disorder:
589 a meta-analysis. *Biological Psychiatry*. 2020 May 1;87(9):S290.
- 590 79. Manoliu A, Meng C, Brandl F, Doll A, Tahmasian M, Scherr M, Schwerthöffer D, Zimmer C, Förstl H,
591 Bäuml J, Riedl V. Insular dysfunction within the salience network is associated with severity of symptoms
592 and aberrant inter-network connectivity in major depressive disorder. *Frontiers in human neuroscience*.
593 2014 Jan 21;7:930.
- 594 80. Tang, S., Li, H., Lu, L., Wang, Y., Zhang, L., Hu, X., ... & Huang, X. (2019). Anomalous functional
595 connectivity of amygdala subregional networks in major depressive disorder. *Depression and*
596 *Anxiety*, 36(8), 712-722.
- 597 81. Ramasubbu R, Konduru N, Cortese F, Bray S, Gaxiola-Valdez I, Goodyear B. Reduced intrinsic
598 connectivity of amygdala in adults with major depressive disorder. *Frontiers in psychiatry*. 2014 Feb
599 19;5:17.
- 600 82. Rolls ET, Treves A. The neuronal encoding of information in the brain. *Progress in neurobiology*. 2011
601 Nov 1;95(3):448-90.
- 602 83. Yanagita T, Maruta T, Uezono Y, Satoh S, Yoshikawa N, Nemoto T, Kobayashi H, Wada A. Lithium

- 603 inhibits function of voltage-dependent sodium channels and catecholamine secretion independent of
604 glycogen synthase kinase-3 in adrenal chromaffin cells. *Neuropharmacology*. 2007 Dec 1;53(7):881-9.
- 605 84. Föhr KJ, Rapp M, Fauler M, Zimmer T, Jungwirth B, Messerer DA. Block of voltage-gated sodium
606 channels by aripiprazole in a state-dependent manner. *International Journal of Molecular Sciences*. 2022
607 Oct 25;23(21):12890.
- 608 85. Szulczyk B, Nurowska E. Valproic acid inhibits TTX-resistant sodium currents in prefrontal cortex
609 pyramidal neurons. *Biochemical and biophysical research communications*. 2017 Sep 16;491(2):291-5.
- 610 86. Gottschalk MG, Leussis MP, Ruland T, Gjeluci K, Petryshen TL, Bahn S. Lithium reverses behavioral and
611 axonal transport-related changes associated with ANK3 bipolar disorder gene disruption. *European*
612 *Neuropsychopharmacology*. 2017 Mar 1;27(3):274-88.
- 613 87. Huang X, Lei Z, El-Mallakh RS: Lithium normalizes elevated intracellular sodium. *Bipolar Disord* 2007
614 May;9(3):298-300.
- 615 88. Jing Y, Zhao N, Deng XP, Feng ZJ, Huang GF, Meng M, Zang YF, Wang J. Pregenual or subgenual anterior
616 cingulate cortex as potential effective region for brain stimulation of depression. *Brain and Behavior*. 2020
617 Apr;10(4):e01591.
- 618 89. Fu Y, Long Z, Luo Q, Xu Z: Functional and structural connectivity between the left dorsolateral
619 prefrontal cortex and insula could predict the antidepressant effects of repetitive transcranial magnetic
620 stimulation. *Front Neuroscience* 2021 Mar; 15: 26.
- 621 90. Chen FJ, Gu CZ, Zhai N, Duan HF, Zhai AL, Zhang X. Repetitive transcranial magnetic stimulation
622 improves amygdala functional connectivity in major depressive disorder. *Frontiers in Psychiatry*. 2020 Jul
623 31;11:732.

624 91. Downar J, Blumberger DM, Daskalakis ZJ: The neural crossroads of psychiatric illness: an emerging
625 target for brain stimulation. Trends in Cognitive Sciences 2016; 20:2149.

626 92. Gellersen HM, Kedzior KK. Antidepressant outcomes of high-frequency repetitive transcranial
627 magnetic stimulation (rTMS) with F8-coil and deep transcranial magnetic stimulation (DTMS) with H1-coil
628 in major depression: a systematic review and meta-analysis. BMC Psychiatry. 2019 Dec;19:1-20.

629 93. Feighner JP, Robins E, Guze SB, Woodruff RA, Winokur G, Munoz R. Diagnostic criteria for use in
630 psychiatric research. Archives of general psychiatry. 1972 Jan 1;26(1):57-63.

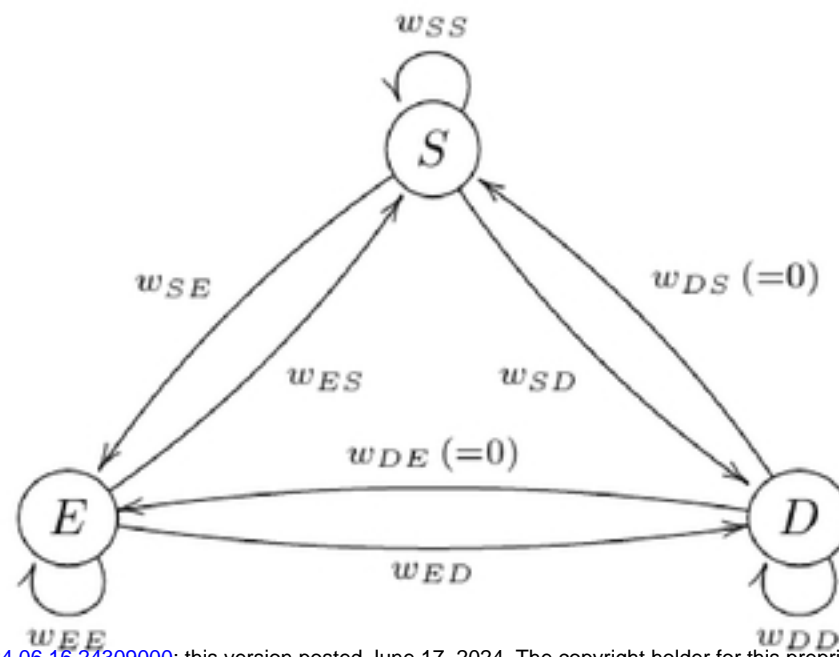
631 94. Cohen BM, Öngür D. The need for evidence-based updating of ICD and DSM models of psychotic and
632 mood disorders. Molecular Psychiatry. 2023 Jan 25:1-3.

633 95. Jakubovski E, Bloch MH. Prognostic subgroups for citalopram response in the STAR* D trial. The
634 Journal of clinical psychiatry. 2014 May 27;75(7):15717.

635

636

637



medRxiv preprint doi: <https://doi.org/10.1101/2024.06.16.24309000>; this version posted June 17, 2024. The copyright holder for this preprint (which was not certified by peer review) is the author/funder, who has granted medRxiv a license to display the preprint in perpetuity. It is made available under a [CC-BY 4.0 International license](https://creativecommons.org/licenses/by/4.0/).

Fig 1. tiff

Fig 2. tiff

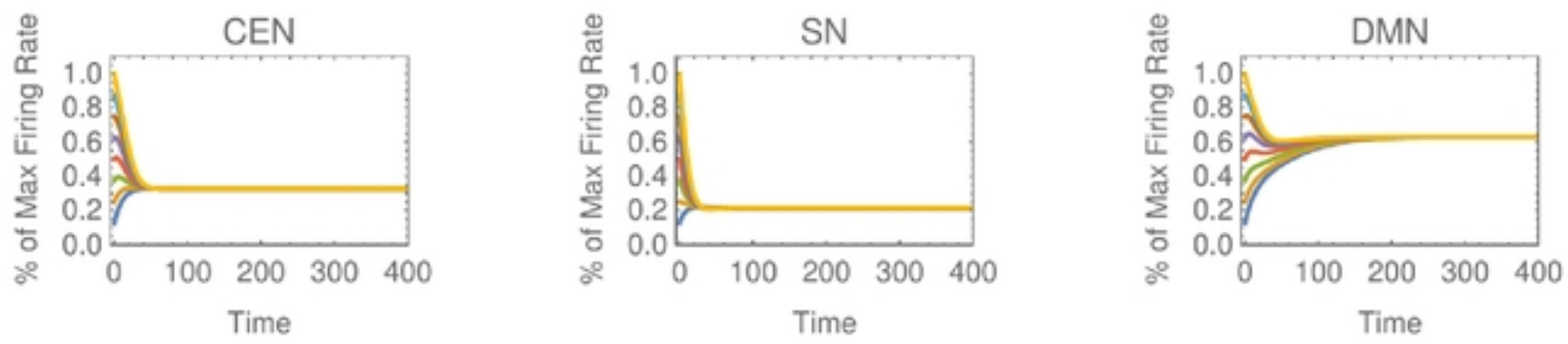


Fig 3. tiff

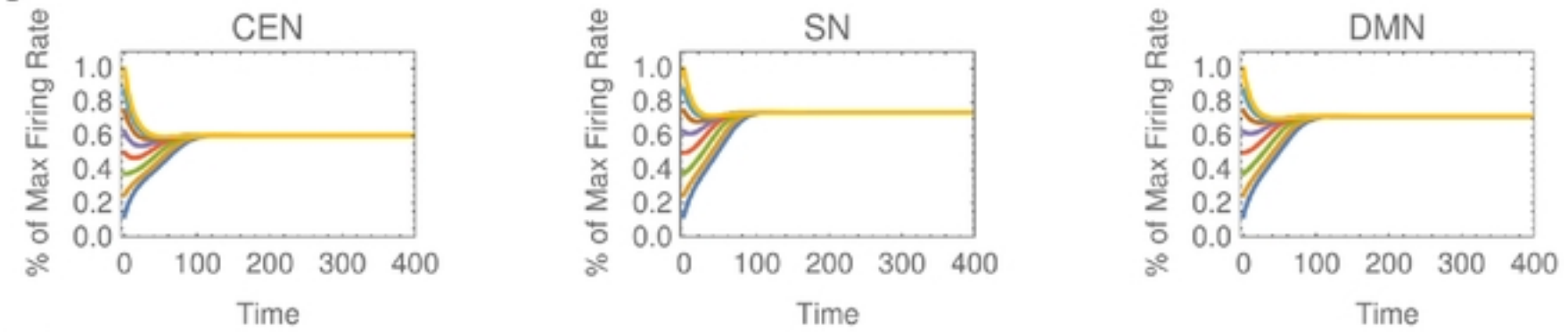


Fig 4. tiff

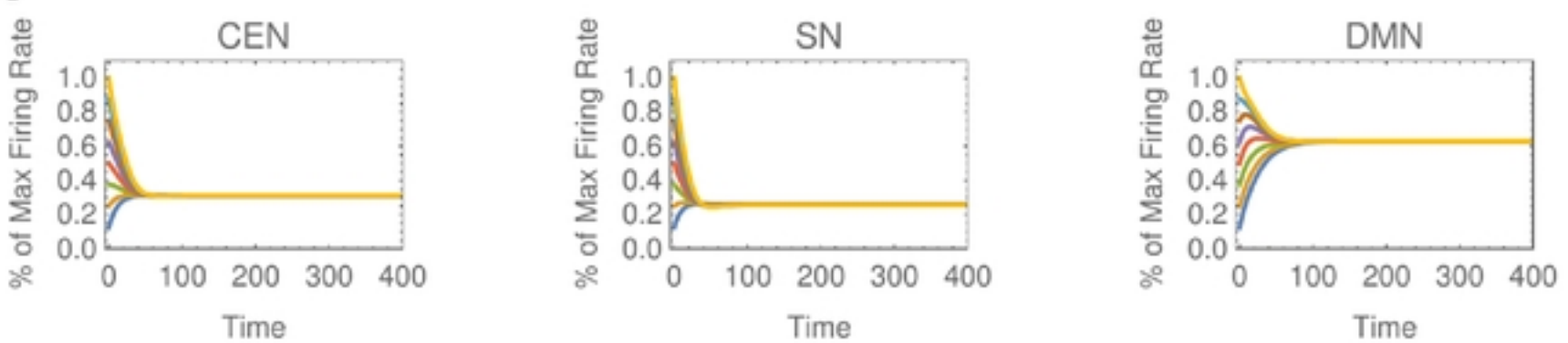


Fig 5.tiff

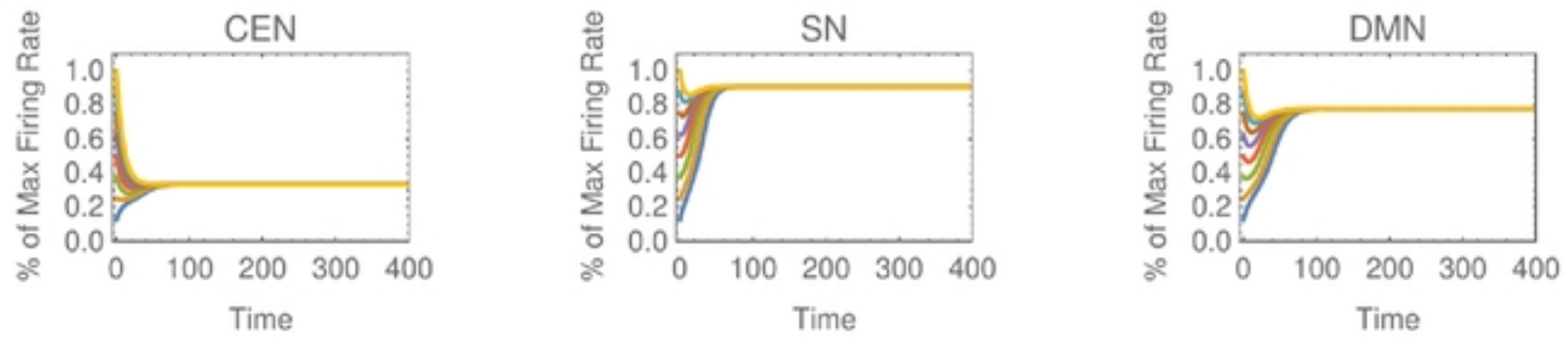
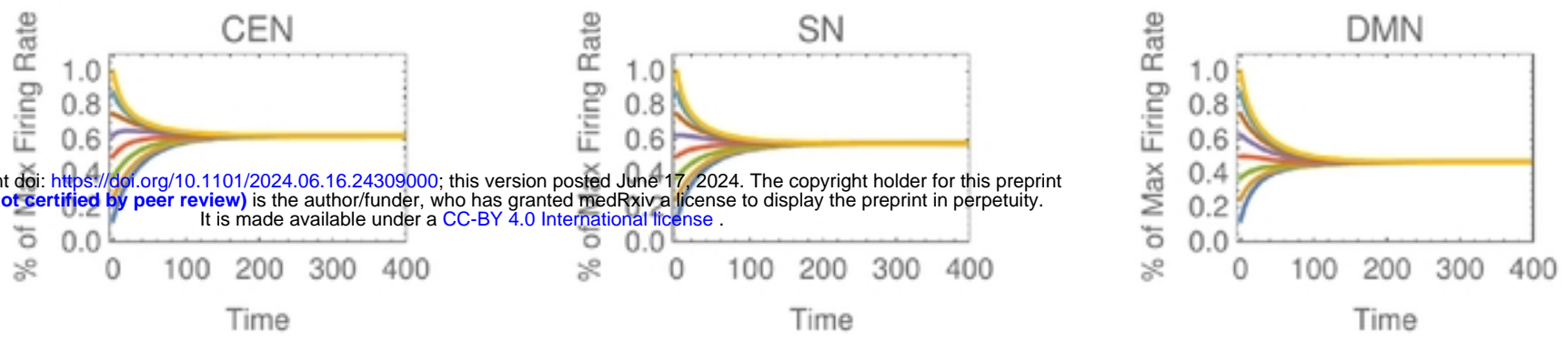


Fig 6. tiff



medRxiv preprint doi: <https://doi.org/10.1101/2024.06.16.24309000>; this version posted June 17, 2024. The copyright holder for this preprint (which was not certified by peer review) is the author/funder, who has granted medRxiv a license to display the preprint in perpetuity. It is made available under a [CC-BY 4.0 International license](https://creativecommons.org/licenses/by/4.0/).